Article | Received 3 April 2026; Revised 27 August 2026; Accepted 23 September 2026; Published 28 September 2026
https://doi.org/10.55092/exrna20260014

Circulating extracellular vesicle miRNAs for distinguishing prostate cancer from benign prostatic hyperplasia

Ting Ding[1,2], Xin Zhang[3] and Lijuan Yu[3,4,*]

[1] Department of Laboratory Medicine, The Second Hospital Affiliated to Xi'an Jiaotong University, Xi'an Jiaotong University, Xi'an, China
[2] Department of Laboratory Medicine, Xijing Hospital, Fourth Military Medical University (Air Force Medical University), Xi'an, China
[3] Department of Laboratory Medicine, Guangdong Provincial Key Laboratory of Precision Medical Diagnostics, Guangdong Engineering and Technology Research Center for Rapid Diagnostic Biosensors, Guangdong Provincial Key Laboratory of Single-cell and Extracellular Vesicles, Nanfang Hospital, Southern Medical University, Guangzhou, China
[4] Sahlgrenska Center for Cancer Research, Department of Surgery, Institute of Clinical Sciences, Sahlgrenska Academy, University of Gothenburg, Gothenburg, Sweden

* Correspondence author; E-mail: ylj185@163.com.

Highlights:

- A three-miRNA panel (miR-92a-1-5p, miR-375, miR-148a-3p) was quantified in plasma EVs using digital PCR.
- The combined miRNA panel achieved an AUC of 0.736 for distinguishing PCa from BPH.
- miR-375 alone showed good diagnostic performance (AUC = 0.735) for identifying bone-metastatic PCa from BPH.
- The panel demonstrated potential as an auxiliary diagnostic tool for PCa but lacked specificity for staging.
- This study validates EV-derived miRNAs as promising non-invasive biomarkers for PCa diagnosis.

Abstract: Aim: Our previous studies identified three extracellular vesicle derived microRNAs (miR-92a-1-5p, miR-375 and miR-148a-3p) potentially associated with prostate cancer (PCa), particularly in advanced stages such as bone-metastatic PCa. This study aimed to evaluate their clinical diagnostic utility as a panel derived from plasma extracellular vesicles. Methods: A total of 49 treatment-naive participants, including 21 with benign prostatic hyperplasia (BPH), 15 with localized PCa, and 13 with bone-metastatic PCa, were enrolled. Plasma extracellular vesicles were isolated, and absolute quantification of the three miRNAs was performed using digital polymerase chain reaction (PCR). Their individual and combined diagnostic performance for distinguishing PCa from BPH and identifying bone metastasis was assessed. Results: Among the three miRNAs, miR-92a-1-5p and miR-375 showed a statistically significant difference in expression between PCa and BPH. The combined three-miRNA panel achieved an improved area under the curve (AUC) of 0.736, representing an enhancement over single markers

and outperforming serum prostate-specific antigen (PSA) (AUC = 0.682) in this cohort. The panel yielded an AUC of 0.766 for detecting bone-metastatic PCa *versus* BPH, but showed limited ability to discriminate localized from metastatic disease. Conclusion: These preliminary findings suggest that the plasma extracellular vesicle-derived three-miRNA panel has auxiliary diagnostic value for differentiating prostate cancer from benign prostatic hyperplasia, and may serve as a supplementary tool to serum PSA.

Keywords: prostate cancer; extracellular vesicles; miRNA; diagnosis

1. Introduction

Prostate cancer (PCa) is a leading malignancy in men [1]. A pressing clinical challenge is the accurate differentiation of PCa from highly prevalent benign prostatic hyperplasia (BPH), as both conditions commonly present with elevated serum prostate-specific antigen (PSA). As the conventional screening biomarker, PSA lacks sufficient specificity for this distinction, resulting in widespread unnecessary biopsies and diagnostic delays [2]. This creates an urgent demand for novel non-invasive biomarkers to complement PSA and improve diagnostic accuracy.

Circulating extracellular vesicles (EVs) have emerged as a promising platform for non-invasive cancer diagnosis and prognosis [3]. EVs are membrane-bound nanoparticles stably present in plasma, whose molecular cargo reflects the pathophysiological state of their parent cells [4]. Current comparative literature indicates that EV-encapsulated microRNAs (miRNAs) exhibit better stability and tissue specificity than free circulating nucleic acids, and accumulating studies have confirmed their value in distinguishing malignant from benign lesions and identifying metastatic disease across multiple tumor types [5,6]. Meanwhile, technical variability in EV isolation methods and a lack of uniform quantification standards remain common limitations in this field.

The three miRNAs investigated in this study (miR-92a-1-5p, miR-375 and miR-148a-3p) were initially screened via high-throughput sequencing in our prior work, all of which are involved in PCa development [7]. miR-148a-3p is dysregulated in PCa and participates in regulating tumor cell biological behaviors [8,9]. miR-375 is associated with PCa progression and aggressive phenotypes [10,11]. miR-92a-1-5p is implicated in PCa tumorigenesis [12–15]. The three miRNAs can provide complementary biological information, and their combined detection may improve diagnostic performance relative to single markers. However, the clinical diagnostic value of this three-miRNA panel in plasma EVs, particularly for differentiating PCa from BPH and detecting bone metastasis, remains unvalidated. Accordingly, this study performed absolute quantification of these miRNAs via digital PCR in plasma EVs from patients with BPH, localized PCa and bone-metastatic PCa, to evaluate their individual and combined diagnostic efficacy.

2. Methods

2.1. Patients

With informed consent from all subjects and approval from the hospital's ethics committee (No. KY20212016-C-1), a total of 49 treatment-naive patients were recruited from the Department of Urology, the First Affiliated Hospital of the Air Force Medical University. All participants were histologically confirmed to have no other concurrent malignancies, and had not received any anti-tumor treatment or prostate-related invasive procedures prior to sample collection.

This study was designed as a cross-sectional diagnostic study aiming to evaluate the differential diagnostic performance of biomarkers. The cohort was divided into three groups: 21 patients with BPH, 15 patients with localized PCa, and 13 patients with bone-metastatic PCa. The staging and risk stratification of PCa patients followed the classification criteria in the European Society for Medical Oncology (ESMO) Clinical Practice Guidelines and European Association of Urology (EAU) Guidelines for prostate cancer [16,17]. A few patients lacked initial PSA value due to incomplete clinical documentation. Detailed clinical characteristics of all subjects are summarized in Table 1.

2.2. Plasma isolation

First, ethylenediaminetetraacetic acid (EDTA) anticoagulated blood samples collected under fasting conditions were centrifuged at 3000 g for 10 minutes at room temperature within 4 hours to separate the plasma. Subsequently, the supernatant was collected after centrifugation at 10,000 g for 10 minutes at room temperature, aliquoted, and stored at −80 °C.

2.3. EVs isolation and characterization

Prostate plasma EVs were isolated from plasma samples using the Exosome Isolation Kit (Yugongbiomed, Shanghai, China) according to the manufacturer's protocols. Briefly, plasma was pre-centrifuged to remove cells and debris, then mixed with the isolation reagent and incubated at 4 °C. After recovery of the EV pellet through centrifugation, the precipitates were further purified using the provided purification columns to ensure high purity of the isolated vesicles.

2.4. EVs characterization

The morphology of EVs was analyzed using transmission electron microscopy (TEM) (Tecnai, USA), as previously described [18]. To examine the size distribution and particle concentration of EVs, fractionated samples were diluted in phosphate-buffered saline (PBS) for nanoparticle tracking analysis (NTA) using a ZetaView instrument (Particle Metrix, Germany). Western blotting (WB), following previous literature [19], was used to detect two EV-positive markers and one EV-negative marker: TSG101 (Abcam ab125011, 1:1000) and CD9 (Abcam ab263019, 1:1000). Calnexin was purchased from Proteintech (10427-2, 1:500 dilution).

2.5. miRNA detection

RNA was extracted from the isolated EVs using the miRNeasy Mini Kit (Qiagen, Hilden, Germany) following the manufacturer's instructions, and then using the PrimeScript™ RT reagent Kit (Takara Bio, Shiga, Japan) according to the manufacturer's instructions for complementary DNA (cDNA) synthesis. The absolute quantification of miRNA was subsequently performed using the naica® Crystal Digital PCR system (Stilla Technologies, Villejuif, France). The 25 µL reaction mixture consisted of 1× naica® EvaGreen PCR MIX (Stilla Technologies), 200 nM of each forward and reverse primer (RiboBio, Guangzhou, China), and 2 µL of the cDNA template. The mixture was loaded into the Sapphire Chips, and the chips were placed into the Geode device. The integrated program performed droplet generation followed by thermal cycling: initial denaturation at 95 °C for 2 min, followed by 45 cycles of 95 °C for

5 s and 60 °C for 30 s [20]. After amplification, the chips were transferred to the Prism reader for six-channel fluorescence detection. The raw data were analyzed using Crystal Miner software (Stilla Technologies) to calculate the absolute concentration of target miRNA, expressed as copies/μL of cDNA, without normalization to EV particle number or protein content.

2.6. Statistical analysis

Statistical analyses were performed using GraphPad Prism (version 9.0). Normally distributed continuous variables are presented as mean ± standard deviation, while non-normally distributed variables (including serum PSA and miRNA expression levels) are presented as median with IQR. Comparisons between two groups were performed using the independent samples t test (normally distributed data) or the Mann–Whitney U test (non-normally distributed data), and comparisons among multiple groups were performed using one-way ANOVA or the Kruskal–Wallis test, as appropriate. Receiver operating characteristic (ROC) curves were constructed, and the area under the curve (AUC) with 95% confidence interval (CI) was calculated. The combined diagnostic performance of the three miRNAs was assessed via logistic regression. Their absolute quantification values served as independent variables to generate predicted probabilities, which were then utilized to construct the combined ROC curve. P-value < 0.05 was considered statistically significant (*, $P < 0.05$; **, $P < 0.01$; ***, $P < 0.001$).

3. Results

3.1. Isolation and characterization of plasma EVs

The basic clinical information of patients is presented in Table 1. Plasma EVs were successfully isolated from all patient cohorts. Transmission electron microscopy revealed that the isolated particles exhibited the typical cup-shaped morphology characteristic of EVs (Figure 1a). Nanoparticle tracking analysis confirmed their size distribution, with a predominant peak around 120 nm (Figure 1b). Western blot analysis further validated the EV identity, demonstrating positive expression of the canonical EV markers CD9 and TSG101, while the endoplasmic reticulum contaminant marker Calnexin was absent (Figure 1c). Collectively, these data confirm the successful isolation of high-purity plasma EVs suitable for downstream miRNA analysis.

Table 1. Basic clinical information of patients.

Patient characteristics	BPH	localized PCa	Bone metastasis PCa
Number of patients	21	15	13
Age	69.1 ± 9.6	74.2 ± 14.5	70.7 ± 9.8
PSA	9.47 (6.96–15.84)	9.96 (6.09–33.19)	33.20 (15.00–713.70)
Gleason Score			
≤ 7	-	10	0
> 7	-	5	13
ISUP Score			
< 3	-	7	0
≥ 3	-	8	13

Age is presented as mean ± SD; PSA is presented as median (interquartile range (IQR)) due to its skewed distribution; ISUP, International Society of Urological Pathology.

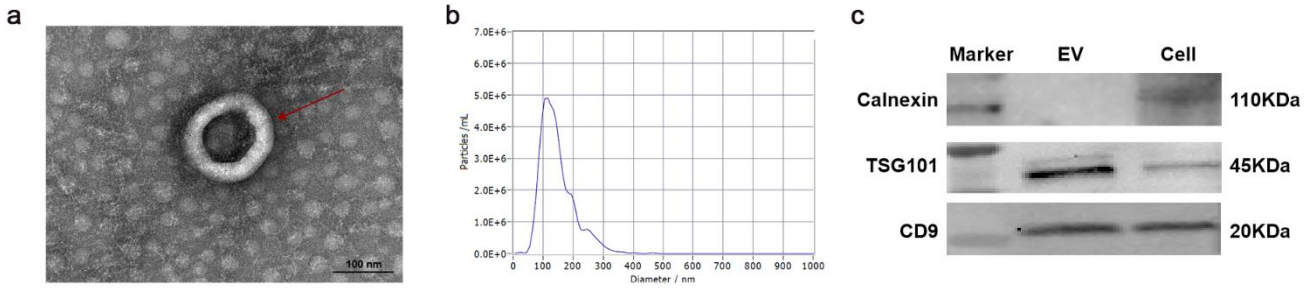

Figure 1. Isolation and characterization of EVs. **(a)** Representative TEM images of EVs, with a scale bar of 100 nm; **(b)** NTA illustrating the size distribution of EVs; **(c)** Western blot analysis depicting the relative expression levels of EV protein markers (CD9, TSG101) alongside the negative control (Calnexin).

3.2. Individual and combined diagnostic performance of the miRNA panel

To evaluate the diagnostic potential of the three miRNAs for prostate cancer, we first assessed their individual performance in distinguishing patients with PCa (including both localized and bone-metastatic disease) from those with BPH. While all three miRNAs displayed a trend of upregulation in the PCa group, miR-92a-1-5p and miR-375 showed statistically significant differences in expression between PCa and BPH (Mann–Whitney U test, P = 0.047 and P = 0.031, respectively), whereas miR-148a-3p did not reach statistical significance (P = 0.149, Figure 2a–c). Correspondingly, when analyzed individually via ROC curves, none of the miRNAs achieved a satisfactory AUC value for diagnosis (Figure 2d–f). Notably, the combined analysis of all three miRNAs (miR-92a-1-5p, miR-375, and miR-148a-3p) markedly improved diagnostic performance, yielding an AUC of 0.736 (95% CI: 0.5979–0.8749, Figure 2g). This result indicates that the synergistic use of this miRNA panel holds superior potential for distinguishing PCa from BPH compared to any single miRNA alone. To confirm the clinical advantage of this panel, we directly compared its performance with the standard clinical biomarker, PSA. As shown in Supplementary Figure S1, serum PSA levels showed no statistically significant difference between the overall PCa and BPH groups (Supplementary Figure S1a). Consequently, its ROC analysis yielded a diagnostic efficacy (AUC = 0.682, 95% CI: 0.4992–0.8655, Supplementary Figure S1b) that was substantially inferior to the performance of our combined three-miRNA panel.

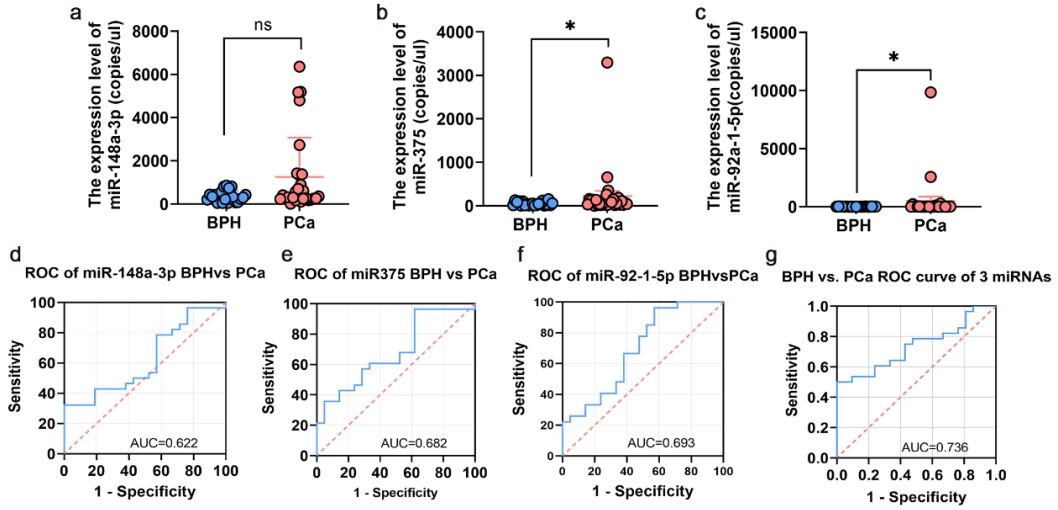

Figure 2. Evaluation of the diagnostic efficacy of three miRNAs for BPH and PCa. **(a)** The expression levels of miR-148a-3p in BPH and PCa; **(b)** The expression levels of miR-375 in BPH and PCa; **(c)** The expression levels of miR-92a-1-5p in BPH and PCa; **(d)** ROC curve for miR-148a-3p in distinguishing between BPH and PCa, AUC = 0.622 (95% CI: 0.4639–0.7810); **(e)** ROC curve for miR-375 in distinguishing between BPH and PCa, AUC = 0.682 (95% CI: 0.5315–0.8324); **(f)** ROC curve for miR-92a-1-5p in distinguishing between BPH and PCa, AUC = 0.693 (95% CI: 0.5393–0.8469); **(g)** ROC curve for the combined diagnostic capability of the three miRNAs in differentiating PCa from BPH, AUC = 0.736 (95% CI: 0.5979–0.8749). **(a–c)** Data were analyzed using Mann–Whitney U test; *, $P < 0.05$.

3.3. Potential in differentiating bone metastatic PCa

We further evaluated the ability of the three miRNAs to identify bone-metastatic PCa by stratifying the cohort into three diagnostic groups: BPH, localized PCa, and bone-metastatic PCa. Analysis of individual miRNAs revealed that while all three were upregulated in localized PCa compared to BPH, their expression levels showed a slight downward trend in bone-metastatic cases (Supplementary Figure S2a–c). Among them, miR-375 exhibited the most promising performance for distinguishing bone-metastatic PCa from BPH, yielding an AUC of 0.736 (95% CI: 0.5668–0.9057) in the ROC analysis (Supplementary Figure S2d).

The combined diagnostic model based on the three-miRNA panel demonstrated enhanced discriminatory power. It achieved an AUC of 0.737 (95% CI: 0.5578–0.9152) for distinguishing localized PCa from BPH (Figure 3a) and an AUC of 0.766 (95% CI: 0.5906–0.9406) for distinguishing bone-metastatic PCa from BPH (Figure 3b). However, the model did not show significant diagnostic value for differentiating between localized PCa and bone-metastatic PCa (AUC = 0.502, 95% CI: 0.2838–0.7214, Figure 3c), indicating its primary utility lies in distinguishing malignant from benign disease rather than in staging advanced PCa.

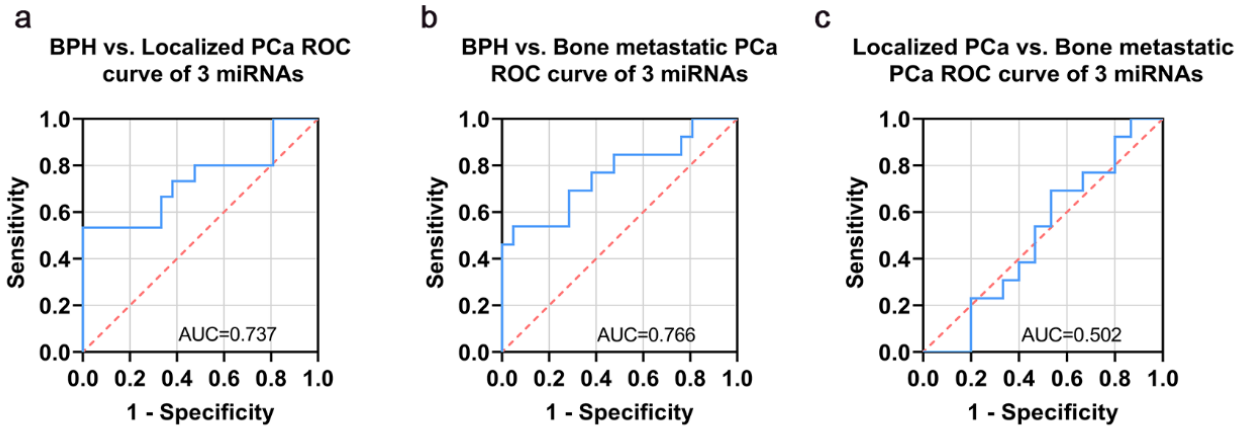

Figure 3. The diagnostic potential of the three miRNAs for prostate conditions. **(a)** ROC curve for the combined diagnostic capability of three miRNAs in differentiating localized PCa from BPH, AUC = 0.737 (95% CI: 0.5578–0.9152); **(b)** ROC curve for the combined diagnostic capability of three miRNAs in differentiating bone metastatic PCa from BPH, AUC = 0.766 (95% CI: 0.5906–0.9406); **(c)** ROC curve for the combined diagnostic capability of three miRNAs in differentiating bone metastatic PCa from localized PCa, AUC = 0.502 (95% CI: 0.2838–0.7214).

4. Discussion

While previous mechanistic studies, including our own, have implicated miRNAs such as miR-92a-1-5p, miR-375, and miR-148a-3p in the pathogenesis of PCa [13,14,21,22], their translational value as clinically applicable biomarkers remain unclear. To bridge this gap, this study aimed to validate the diagnostic potential of a plasma EVs-derived miRNA panel, focusing on its ability to distinguish PCa from BPH and to identify bone-metastatic disease.

This study's methodology is based on effectively isolating plasma EVs using a commercial kit. We confirmed the EVs' typical morphology, size (~120 nm), and marker expression (CD9, TSG101) without Calnexin contamination through electron microscopy, nanoparticle tracking, and western blot. This isolation is crucial for accurate miRNA analysis, ensuring reliable digital PCR results and strengthening our diagnostic conclusions.

Individually, miR-92a-1-5p, miR-375, and miR-148a-3p lack sufficient diagnostic power to differentiate PCa from BPH. Although miR-148a-3p did not reach statistical significance individually in this specific cohort, it was purposefully retained in the combined panel based on its pre-identified biological relevance from our prior high-throughput sequencing analysis. In multivariate modeling, such variables often provide complementary diagnostic information. Consequently, when combined, they achieve a significantly better AUC of 0.736, indicating the advantage of multi-miRNA panels over single markers. This combination may serve as a useful diagnostic tool alongside serum PSA testing, especially when PSA results are unclear, potentially reducing unnecessary biopsies. The study highlights the difficulty of identifying a single effective biomarker for PCa and supports the use of multiple biomarkers for more accurate diagnosis.

There are also some studies that have explored the value of these miRNAs in PCa. Several studies have confirmed that miR-92a is upregulated in PCa [12–15]. However, these studies were all conducted on tissue or cell models. Our research is one of the first studies to demonstrate the diagnostic value of plasma exosomal miR-92a-1-5p for PCa. Regarding miR-148, Coradduzza *et al.* demonstrated its downregulation in PCa tissues and its role in cancer progression [8,9]. This apparent discrepancy in directionality—downregulation in tumor tissues but upregulation in plasma EVs observed in our study—can be explained by the selective sorting mechanism of EVs. Previous studies have reported that cancer cells actively and selectively package specific miRNAs into EVs, resulting in EV miRNA profiles that are distinct from those of their parent cells [23]. This is a broadly observed, actively regulated process governed by RNA-binding proteins and specific sequence motifs that direct cargo sorting, although the repertoire of selectively packaged miRNAs varies depending on cell type and activation state [24,25]. This active efflux decreases the intracellular concentration of tumor-suppressive factors such as miR-148a-3p in tumor cells and may subsequently affect cancer progression. Whether this selective packaging represents a general disposal mechanism for tumor-suppressive miRNAs across cancer types or is specific to miR-148a-3p in the PCa context remains an open question. Future comparative studies across different cancers will be needed to delineate the generality *versus* context specificity of this mechanism. Previous studies mainly explored the diagnostic value of overall plasma miR-148 rather than EV-encapsulated miR-148a-3p, and did not analyze its potential in differentiating PCa bone metastasis. For miR-375, numerous studies have confirmed its diagnostic value in PCa [13,10,11], and it has been found to be associated with the poor prognosis of PCa [22,26,27]. However, most of these

studies were conducted using tissue or cell models, and no study has explored the value of plasma EV miR-375 in PCa bone metastasis. Our study also found that miR-375 exhibits good diagnostic performance (AUC = 0.736) for PCa bone metastasis detection from BPH, indicating its potential as a key biomarker. Literature supports that miR-375 promotes PCa cell migration and induces docetaxel resistance by targeting YAP124,26. Moreover, exosomal miR-375 is significantly elevated in bone-metastatic tumors and contributes to the formation of a pre-metastatic niche in bone [25]. These mechanisms likely underlie its high diagnostic value, linking its expression to bone-metastasis-related pathways.

Furthermore, our three-miRNA panel showed a complex pattern in staging: all miRNAs were higher in localized PCa than in BPH but decreased in bone-metastatic disease. This suggests a shift in EV-miRNA cargo during disease progression, possibly due to changes in tumor cell behavior or interactions with the bone microenvironment. The downregulation of these miRNAs in bone metastases may indicate a reprogramming of EV cargo by PCa cells, shifting from a “pro-growth” to a “niche adaptation” or “systemic crosstalk” role [7]. This dynamic change in miRNA profiles may explain why our panel, designed for malignancy detection, lacks specificity in distinguishing localized from metastatic disease, aligning with new insights into selective EV cargo sorting.

However, the model did not demonstrate effective diagnostic performance in distinguishing between localized PCa and bone-metastatic PCa. This limitation may stem from several factors. First, the small sample size and lack of an independent validation cohort may overestimate the panel’s diagnostic performance. Although strictly enrolling treatment-naive patients eliminates therapeutic confounding—making this cohort highly informative—it inherently restricts sample size, necessitating cautious interpretation of these preliminary findings. Second, although the three selected miRNAs showed overall upregulation in malignant disease, their dynamic changes during disease progression may not sensitively reflect the molecular differences between localized progression and distant metastasis. Third, although the initial plasma input volume was strictly standardized, our absolute quantification lacked normalization to EV particle number or protein content. To mitigate potential biases from inter-individual variations in circulating EV concentrations, future studies should incorporate EV-specific normalization. Furthermore, the formation of bone metastasis in prostate cancer involves complex remodeling of the tumor microenvironment and systemic regulation; a single plasma EV miRNA profile may not fully capture the key biological characteristics of this process. Therefore, the current model is more suitable for assisting in the differentiation of benign and malignant prostate conditions, while it still has clear shortcomings in precise staging.

Future research could further optimize model construction by expanding sample sizes, incorporating novel biomarkers with greater staging specificity, and adopting multi-omics analysis strategies, thereby advancing its application in the precise diagnosis and stratified management of PCa.

5. Conclusion

Collectively, these preliminary findings suggest that a three-miRNA signature (miR-92a-1-5p, miR-375, and miR-148a-3p) from plasma extracellular vesicles may help differentiate prostate cancer from benign prostatic hyperplasia, with a combined AUC of 0.736. The panel also improves detection of bone-metastatic prostate cancer (AUC = 0.766) but lacks specificity for distinguishing localized from metastatic disease. These results underscore the potential of EV-based liquid biopsy and the need for further biomarker refinement for precise prostate cancer stratification.

Data availability statement

All the original data are available upon reasonable request for correspondence author. And a supplementary file is provided with this article. This supplementary material shows the diagnostic value of PSA and three EV miRNAs in distinguishing benign prostate hyperplasia from prostate cancer.

Declaration of generative AI and AI-assisted technologies

During the preparation of this manuscript, the authors used generative AI tools only to improve language and readability. Specifically, the authors used ChatGPT for language polishing only entire manuscript. The authors take full responsibility for the content of the manuscript.

Acknowledgments

This work was supported by the Shaanxi Provincial Natural Science Basic Research Program to T.D. [under Grant No. 2025JC-YBQN-1185], the National Natural Science Foundation of China to L.Y. [under Grant No. 82203711] and the China Postdoctoral Science Foundation to L.Y. [under Grant No. 2021M701631].

Authors' contribution

Conceptualization, L.Y.; methodology, T.D. and L.Y.; formal analysis, T.D.; investigation, T.D.; data curation, T.D.; writing—original draft preparation, T.D.; writing—review and editing, X.Z. and L.Y.; supervision, L.Y.; project administration, L.Y.; funding acquisition, T.D. and L.Y. All authors have read and agreed to the published version of the manuscript.

Conflicts of interest

All authors declare that there are no conflicts of interest.

Ethical statement

This study was conducted in accordance with the principles of the Declaration of Helsinki and approved by the ethics committee of the Xijing Hospital affiliated to Air Force Medical University (No. KY20212016-C-1). The samples and clinical information were obtained with the patient's written informed consent.

References

[1] Siegel RL, Kratzer TB, Giaquinto AN, Sung H, Jemal A. Cancer statistics, 2025. *CA Cancer J. Clin.* 2025, 75(1):10–45.

[2] Liu J, Dong L, Zhu Y, Dong B, Sha J, *et al.* Prostate cancer treatment—China's perspective. *Cancer Letters* 2022, 550:215927.

[3] Robinson H, Roberts MJ, Gardiner RA, Hill MM. Extracellular vesicles for precision medicine in prostate cancer—is it ready for clinical translation? *Semin. Cancer Biol.* 2023, 89:18–29.

[4] Batool SM, Yekula A, Khanna P, Hsia T, Gamblin AS, *et al.* The Liquid Biopsy Consortium: challenges and opportunities for early cancer detection and monitoring. *Cell Rep. Med.* 2023, 4(10):101198.

[5] Wang X, Zhang L, Cheng L, Wang Y, Li M, *et al.* Extracellular vesicle-derived biomarkers in prostate cancer care: opportunities and challenges. *Cancer Lett.* 2024, 601:217184.

[6] Zhang C, Qin C, Dewanjee S, Bhattacharya H, Chakraborty P, *et al.* Tumor-derived small extracellular vesicles in cancer invasion and metastasis: molecular mechanisms, and clinical significance. *Mol. Cancer* 2024, 23(1):18.

[7] Yu L, Sui B, Fan W, Lei L, Zhou L, *et al.* Exosomes derived from osteogenic tumor activate osteoclast differentiation and concurrently inhibit osteogenesis by transferring COL1A1-targeting miRNA-92a-1-5p. *J. Extracell. Vesicles* 2021, 10(3):e12056.

[8] Coradduzza D, Cruciani S, Arru C, Garroni G, Pashchenko A, *et al.* Role of miRNA-145, 148, and 185 and stem cells in prostate cancer. *Int. J. Mol. Sci.* 2022, 23(3):1626.

[9] Coradduzza D, Solinas T, Balzano F, Culeddu N, Rossi N, *et al.* miRNAs as molecular biomarkers for prostate cancer. *J. Mol. Diagn.* 2022, 24(11):1171–1180.

[10] He S, Shi J, Mao J, Luo X, Liu W, *et al.* The expression of miR-375 in prostate cancer: a study based on GEO, TCGA data and bioinformatics analysis. *Pathol. Res. Pract.* 2019, 215(6):152375.

[11] Zedan AH, Osther PJS, Assenholt J, Madsen JS, Hansen TF. Circulating miR-141 and miR-375 are associated with treatment outcome in metastatic castration resistant prostate cancer. *Sci. Rep.* 2020, 10(1):227.

[12] Zhang S, Yu J, Sun B, Hou G, Yu Z, *et al.* MicroRNA-92a targets SERTAD3 and regulates the growth, invasion, and migration of prostate cancer cells via the P53 pathway. *OncoTargets Ther.* 2020, 13:5495–5514.

[13] Dal Santo G, Frasca M, Bertoli G, Castiglioni I, Cava C. Identification of key miRNAs in prostate cancer progression based on miRNA-mRNA network construction. *Comput. Struct. Biotechnol. J.* 2022, 20:864–873.

[14] Ashok G, Das R, Anbarasu A, Ramaiah S. Comprehensive analysis on the diagnostic role of circulatory exosome-based miR-92a-3p for osteoblastic metastases in prostate adenocarcinoma. *J. Mol. Recognit.* 2023, 36(8):e3042.

[15] Zheng Y, Yang L, Wu X, Dong Z, Mai H. miR-92a promotes proliferation and inhibits apoptosis of prostate cancer cells through the PTEN/Akt signaling pathway. *Libyan J. Med.* 2021, 16(1):1971837.

[16] Parker C, Castro E, Fizazi K, Heidenreich A, Ost P, *et al.* Prostate cancer: ESMO clinical practice guidelines for diagnosis, treatment and follow-up. *Ann. Oncol.* 2020, 31(9):1119–1134.

[17] Cornford P, Van den Bergh RCN, Briers E, Van den Broeck T, Brunckhorst O, *et al.* EAU-EANM-ESTRO-ESUR-ISUP-SIOG guidelines on prostate cancer-2024 update. Part I: screening, diagnosis, and local treatment with curative intent. *Eur. Urol.* 2024, 86(2):148–163.

[18] Sedej I, Štalekar M, Tušek Žnidarič M, Goričar K, Kojc N, *et al.* Extracellular vesicle-bound DNA in urine is indicative of kidney allograft injury. *J. Extracell. Vesicles* 2022, 11(9):e12268.

[19] Ding T, Diao Y, Fu R, Gong C, He Q, *et al.* The significance of urine extracellular vesicle DNA methylation detection in the diagnosis and classification of prostate cancer. *J. Adv. Res.* 2026, 84:975–989.

[20] Gornalusse G, Spengler RM, Sandford E, Kim Y, Levy C, *et al*. Men who inject opioids exhibit altered tRNA-Gly-GCC isoforms in semen. *Mol Hum Reprod* 2023, 29(3):gaad003.

[21] Yu L, Sui B, Zhang X, Liu J, Hao X, *et al.* miR-92a-1-5p enriched prostate cancer extracellular vesicles regulate osteoclast function via MAPK1 and FoxO1. *J. Exp. Clin. Cancer Res.* 2023, 42(1):109.

[22] Liu Y, Yang C, Chen S, Liu W, Liang J, *et al.* Cancer-derived exosomal miR-375 targets DIP2C and promotes osteoblastic metastasis and prostate cancer progression by regulating the Wnt signaling pathway. *Cancer Gene Ther.* 2023, 30(3):437–449.

[23] Groot M, Lee H. Sorting mechanisms for microRNAs into extracellular vesicles and their associated diseases. *Cells* 2020, 9(4):1044.

[24] Fabbiano F, Corsi J, Gurrieri E, Trevisan C, Notarangelo M, *et al.* RNA packaging into extracellular vesicles: an orchestra of RNA-binding proteins? *J. Extracell. Vesicles* 2020, 10(2):e12043.

[25] Mangiapane G, Notarangelo M, Canarutto G, Fabbiano F, Dalla E, *et al.* The DNA-repair protein APE1 participates with hnRNPA2B1 to motif-enriched and prognostic miRNA secretion. *Oncogene* 2024, 43(24):1861–1876.

[26] Wang Y, Lieberman R, Pan J, Zhang Q, Du M, *et al.* miR-375 induces docetaxel resistance in prostate cancer by targeting SEC23A and YAP1. *Mol. Cancer* 2016, 15(1):70.

[27] Selth LA, Das R, Townley SL, Coutinho I, Hanson AR, *et al.* A ZEB1-miR-375-YAP1 pathway regulates epithelial plasticity in prostate cancer. *Oncogene* 2017, 36(1):24–34.